ISSN 0036-0236, Russian Journal of Inorganic Chemistry, 2012, Vol. 57, No. 10, pp. 1328–1334. © Pleiades Publishing, Ltd., 2012.
Original Russian Text © A.A. Shteinman, 2012, published in Zhurnal Neorganicheskoi Khimii, 2012, Vol. 57, No. 10, pp. 1413–1419.

COORDINATION COMPOUNDS

Structure and Catalytic Activity of a New Iron(II) Complex with a Tetradentate Carboxamide Ligand: The Effect of the Outer-Sphere Donor on the Chemoselectivity of the Metal Complex Catalyst

A. A. Shteinman

Institute of Problems of Chemical Physics, Russian Academy of Sciences, Chernogolovka, Moscow oblast, 142432 Russia
e-mail: as237t@icp.ac.ru

Received February 10, 2011

Abstract—The interaction between $Fe(ClO_4)_2$ or $Fe(OTf)_2(MeCN)_2$ and 2 equiv of the potentially tetradentate ligand bis(2-pyridyl)methyl-2-pyridinecarboxamide ($Py_2CHNHCOPy$, tpcaH) yields the iron(II) complex $[Fe^{II}(tpcaH)_2]X_2$ (X = ClO_4, OTf), in which, according to X-ray crystallography data, tpcaH is facially coordinated to the iron atom as a tridentate ligand through the carbonyl group and two pyridyl donors of the bis(2-pyridyl)methylcarboxamide moiety and the third pyridyl group is uninvolved in coordination. The oxidation of saturated and unsaturated hydrocarbons with hydrogen peroxide involving this complex has been investigated. The presence of the uncoordinated nitrogen donor in the outer coordination sphere of the complex exerts a crucial effect on it catalytic properties.

DOI: 10.1134/S0036023612100129

The catalytic characteristics of a metal complex depend considerably on its ligand structure, since the ligand exposes particular properties of the metal ion. As a consequence, there is a wide diversity of catalysts based on the same metal. The discovery and study of iron-containing oxygenases catalyzing, in biological systems, a variety of selective oxidation processes, such as the hydroxylation of unactivated C–H bonds and the epoxidation and *cis*-dihydroxylation of double bonds, has stimulateda search for similar catalysts of nonbiological origin [1]. The determination of the structure of nonheme iron-containing oxygenases in the last decade has revealed the general structural motif of their active sites, specifically, the facially coordinated triad of two histidines and one carboxylate constituting an N,N,O-donor set [2] (Fig. 1). A complex between iron(II) and bis(2-pyridyl)methylbenzamide, $[Fe(Py_2CHNHCOPh)_2](OTf)_2$ (Fig. 2, complex **1**), was synthesized earlier in order to model the oxygenases [3]. This complex contains a facial N,N,O-donor set and efficiently catalyzes the selective *cis*-dihydroxylation of various alkenes, thus providing a model for the family of mononuclear oxygenase, which are called Rieske oxygenases [4]. The *cis*-dihydroxylation selectivity of this catalyst (diol : epoxide ratio) is 80% for electron donor alkenes and 100% for electron acceptor alkenes. A fairly efficient olefin oxidation catalyst, this complex is almost incapable of catalyzing C–H bond oxidation. For example, cyclohexene hydroxylation at its weakest C–H (in the allylic position) occurs to the extent of a few percent. The problem of finding more effective catalysts for preparative alkene *cis*-dihydroxylation was addressed by investigating the effect of the structure of carboxamide ligands on the catalytic activity of their iron(II) complexes (Fig. 2, complexes **1**–**3**) in the oxidation of electron donor and electron acceptor alkenes with hydrogen peroxide [5]. That study provided evidence that these reactions proceed via a $Fe^{II}Fe^{IV}$ catalytic cycle involving these catalysts, as distinct from the $Fe^{III}Fe^{V}$ catalytic cycle observed for iron complexes with multidentate ligands containing only nitrogen donors [6, 7].

Here, we consider the structure and catalytic activity of an iron(II) complex with the potentially tetradentate ligand bis(2-pyridyl)methyl-2-pyridinecarboxamide ($Py_2CHNHCOPy$, tpcaH, **4**). This ligand

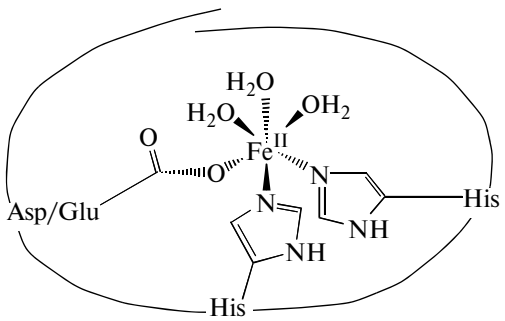

Fig. 1. Active site of iron-containing N,N,O-oxygenases.

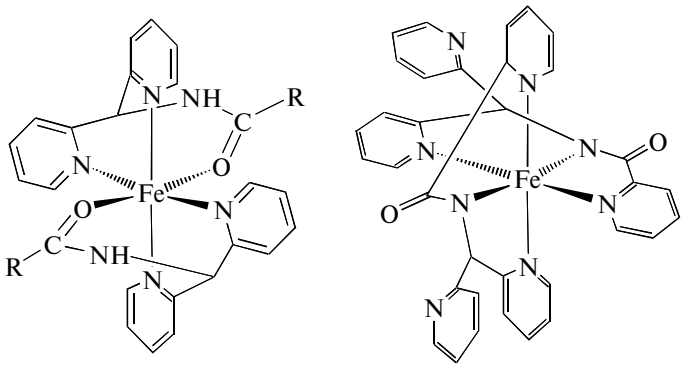

(a) (b)

Fig. 2. (a) Facial and (b) meridional configurations of the carboxamide ligands in complexes **1**–**4**. R = C_6H_5 (**1**), 4-C_6H_4OMe (**2**), 4-$C_6H_4CF_3$ (**3**), and 2-C_5H_4N (**4**).

differs from the above tridentate ligands in that it has a pyridyl radical in place of phenyl at the carbonyl group (Fig. 2a) [8, 9]. The outer-sphere donor effect on the chemoselectivity of the metal complex catalyst was discovered.

EXPERIMENTAL

All solvents were 99.5% or purer. They were used as received or were predried over molecular sieve 3 Å. Hydrocarbons were distilled from sodium metal. The other chemicals were commercial-grade (99%, Aldrich). Iron(II) triflate $Fe^{II}(OTf)_2(MeCN)_2$ was synthesized via a standard procedure [10]. The synthesis was carried out in an argon atmosphere using a glovebox or a Schlenk line.

Elemental analyses were carried out in the Microanalysis Laboratory, Institute of Problems of Chemical Physics, Russian Academy of Sciences. UV–vis absorption spectra were recorded on Specord 75-IR and M-82 spectrophotometers. Electrospray ionization mass spectra (ESI-MS) were obtained on a high-resolution time-of-flight mass spectrometer at the Institute for Energy Problems of Chemical Physics, Russian Academy of Sciences [11]. ^{1}H NMR spectra were taken from solutions in acetonitrile-d_3 on a Varian UNITY spectrometer operating at 300 MHz, with chemical shifts measured relative to the resonance of the residual protons of the solvent.

The structure of complex **4** was determined by X-ray diffraction in the X-ray Crystallographic Laboratory, Department of Chemistry, University of Minnesota, on a Siemens SMART Platform CCD diffractometer (173(2) K, MoK_α radiation, graphite monochromator). The crystal (~0.32 × 0.28 × 0.21 mm) was glued onto the end of a glass capillary 0.1 mm in diameter. The structure determination conditions and crystallographic data are presented in Table 1. The structure was solved using the Sir97 software and was refined with the SHELXR-97 program package. All non-hydrogen atoms were located geometrically and refined anisotropically. All hydrogen atoms were placed in their ideal position and were refined isotopically. The lengths of the bonds between the iron atoms

Table 1. Crystallographic data and X-ray structure determination parameters

Formula	$C_{38}H_{32}Cl_4N_8O_8S_2F_6Fe$
FW	1104.49
System	Monoclinic
Space group	$P2_1/n$
Unit cell parameters	a = 12.652(3) Å $\alpha = 90°$
	b = 15.815(4) Å $\beta = 110.969(5)°$
	c = 12.744(3) Å $\gamma = 90°$
V	2381(1) Å^3
Z	2
ρ_{calc}	1541 g/cm^3
μ	0.0710 cm^{-1}
θ	1.29°–25.09°
Total number of reflections	20 914
Independent reflections	4218 [R(int) = 0.0665]
Observed reflections	3190
Refinement method	Full-matrix least-squares refinement on F^2
GOOF on F^2	0.989
R [$I > 2\sigma(I)$]	$R1$ = 0.1110, $wR2$ = 0.2455

Table 2. Comparison of $r(Fe^{II}$–donor atom) distances (Å) for complexes **1**–**4**, **6*** and **7**** and EDO mononuclear N,N,O-oxygenases (averaged values for 11 structures [13])

Bond	**1**	**2**	**3**	**4**	**6***	**7****	EDO
Fe–O	2.043	2.043	2.047	2.043	2.121	2.228	2.04
Fe–N(2)	2.171	2.167	2.174	2.091	2.147	2.100	2.20
Fe–N(3)	2.181	2.187	2.178	2.214	2.173	2.122	2.27
Δ(FeN(2–3))	0.010	0.020	0.004	0.123	0.026	0.022	0.070

Notes: * $[L_2Fe] \cdot 2D_2O$ (**6**), where L = 3,3-bis(1-methylimidazol-2-yl)propionate [13].
** $[L^1{}_2Fe](BPh_4)_2$ (**7**), where L^1 = propyl 3,3-bis(1-methylimidazol-2-yl)propionate [12].

and the donors of the inner coordination sphere are listed in Table 2.

The oxidation of saturated hydrocarbons in the presence of complex **4** was carried out at 20°C in 10-mL glass vessels [9]. A syringe technique [3] was used in cyclohexene oxidation. The oxidation products were analyzed on a Hewlett Packard 5880A chromatograph with a flame-ionization detector and Carbowax 20M or AT-1 capillary column.

The tpcaH ligand was synthesized via an earlier described procedure [9] and was purified by recrystallization from ethanol; mp 146°C. IR (KBr), ν, cm^{-1}: 3350, 1670 (amide band 1), 1504 (amide band 2).

Synthesis of $[Fe^{II}(tpcaH)_2](ClO_4)_2$ (4-ClO_4). (Attention! Perchlorates are potentially explosive and should be handled with care.) A solution of $Fe(ClO_4)_2 \cdot 6H_2O$ (0.095 g, 0.26 mmol) in MeCN (1 mL) was carefully added to a solution of tpcaH (0.145 g, 0.5 mmol) in 3 mL of MeCN under stirring, and stirring was continued for 2 h. Diethyl ether was added dropwise to the resulting solution until slight opacity, and the solution was left standing overnight in a refrigerator. The next day, the yellow precipitate of **4**-ClO_4 was filtered and vacuum-dried. UV-vis (MeCN), λ_{max}, nm, (ε, M^{-1} cm^{-1}): 270 (25000), 360 (3000), 415 (2400), 800 (100).

Synthesis of $[Fe^{II}(tpcaH)_2](OTf)_2$ (4-OTf). Yellow fine crystals of **4**-OTf were precipitated by stirring $Fe^{II}(OTf)_2(MeCN)_2$ (0.25 mmol) and tpcaH (0.50 mmol) in 5 mL dichloromethane overnight. The precipitate filtered, washed with a small amount of CH_2Cl_2, and vacuum-dried under pumping. Crystals for X-ray crystallography were grown at –25°C using slow pentane diffusion into a solution of **4**-OTf in CH_2Cl_2/MeCN (10 : 1).

UV–vis (MeCN), λ_{max}, nm (ε, M^{-1} cm^{-1}): 265 (20000), 358 (3000), 412 (2500), 800 (100).

IR (KBr), ν, cm^{-1}: 1639, 1602, 1560, 1475, 1445, 1375, 1257, 1163, 1031, 998, 759, 701, 638, 584, 517.

^{1}H NMR (300 MHz, Me_2CO, 25°C), δ, ppm: 9.0, 14.0, 22.5, 35.2, 39.0, 43.2, 60.1, 67.1, 77.0, 80.9. 90.0.

ESI-MS, fragment (X = FeLH, %): $[X(MeCN)]^{2+}$, 24; $[X(MeCN)_2]^{2+}$, 72; $[X(LH)]^{2+}$, 100; $[X(L)]^+$, 43; $[X(LH)(OTf)]^+$, 35.

For $C_{36}H_{28}N_8O_8S_2F_6Fe$ anal. calcd. (%): C, 46.26; H, 3.02; N, 11.99; S, 6.86. Found (%): C, 45.98; H, 3.07; N, 11.92; S, 7.05.

RESULTS AND DISCUSSION

The known model complexes imitating nonheme iron-containing oxygenases have bidentate [12], tridentate [3, 5, 13], tetradentate [14], or pentadentate [15] ligands. The multidentate ligand tpcaH can be tetradentate, tridentate, or bidentate. In the case of the tetradentate or tridentate coordination mode, there can be different sets of donor atoms involved in the inner coordination sphere of the complex [16]. In addition, owing to the presence of the acidic H atom in the carboxamide group, the ligand can coordinate to the iron atom either as a neutral molecule or as an anion (in deprotonated form) [16]. Yellow complexes **4**-ClO_4 and **4**-OTf were synthesized at an iron salt-to-ligand ratio of 1 : 2. As this ratio is increased to 1 : 1, the earlier described orange complex **5** [9] forms as well. Reducing this ratio to 1 : 3 does not lead to the formation of any other complexes. The perchlorate complexes were synthesized in acetonitrile. The best results for the triflate complexes were obtained with CH_2Cl_2. Since the properties of **4**-ClO_4 and **4**-OTf were indistinguishable, both complexes will hereafter be referred to as **4**.

The elemental analysis and mass spectrometric data are consistent with the formula $[Fe^{II}(tpcaH)_2]^{2+}$ for the complex cation. The ^{1}H NMR peaks are narrow and lie within the 9–90 ppm range. Therefore, complex **4** is a high-spin complex of iron(II) [14]. The IR spectrum of the ligand shows characteristic bands of the carboxamide group, namely, a narrow strong band at 3350 cm^{-1} (ν_{NH}) and strong bands at 1670 cm^{-1} (ν_{CO}, amide band 1) and 1504 cm^{-1} (ν_{NH}, amide band 2) [17]. The formation of complex **4** causes a weakening and broadening of the 3350 cm^{-1} band and shifts amide band 1 to a lower frequency of 1639 cm^{-1}. This shift, $\Delta = 31$ cm^{-1}, is in agreement with the shift values observed for other carboxamide complexes [5, 17]. The complexation-induced decrease in ν_{CO} indicates that the carboxamide group of the ligand is coordinated to iron through its carbonyl oxygen atom, since

coordination through the nitrogen atom would increase ν_{CO} because of the disruption of conjugation [18]. In mononuclear complexes, this coordination mode of the carboxamide group renders impossible the coordination of the neighboring pyridyl to the same iron atom. According to spectroscopic data, complex **4** is in the high-spin state. This is quite natural since the carboxamide group is a weak-field ligand. The electronic spectrum of the complex shows two strong bands at 360 and 415 nm, which are consistent with the d^6 electron configuration. The weak band at 830 nm is assigned to the ${}^5T_{2g}$—${}^5E_g$ transition, which is the only spin-allowed transition for the high-spin, octahedrally coordinated d^6 Fe^{2+} ion [19]. The X-ray crystallographic data for **4** confirm the inferences from the spectroscopic studies.

The crystal structure of complex **4**-OTf (Fig. 3) differs significantly from the structure of $[Fe^{II}(tpca)_2]$ synthesized by reacting tpcaH with $[Fe^{II}(MeCOO)_2]$ [16]. The deprotonated carboxamide ligand in the $[Fe^{II}(tpca)_2]$ complex acts as a tridentate meridional ligand (Fig. 2b). Either of the two ligands in this complex is coordinated to iron only through its nitrogen atoms, namely two nitrogen atoms from the structurally nonequivalent pyridyls and one carboxamide nitrogen atom, while one of the pyridyl donors remains uncoordinated. The observed meridional coordination suggests that a planar configuration is favorable for the anionic ligand; however, this configuration prevents the coordination of the third pyridyl. According to X-ray crystallographic data, tpcaH in complex **4** is also a tridentate ligand, but with another set of donor atoms: iron is coordinated with two facial N,N,O-ligands (Fig. 1a), and one of the pyridyls in either ligand is again uncoordinated. Thus, the structure of **4** is similar to the structure of complexes **1**–**3** and differs from the latter in that it has two uncoordinated pyridyls.

The complex cation **4** has an almost ideal octahedral configuration with an iron atom in the inversion center. Its two carboxamide oxygen atoms are *trans* to one another. The relatively short $Fe—O_{amide}$ bond length (2.043 Å) is evidence of strong interaction between the carboxamide oxygen atom and the metal atom, and this is in agreement with the observed complexation-induced decrease in ν_{CO}. The Fe—N bond lengths (Table 2) confirm the high-spin state of iron in **4**. For comparison, we present, un the same table, X-ray crystallographic data for complexes **1**–**4** and for the related complexes **6** and **7** with N,N,O-facial set of donor atoms and averaged bond lengths for 11 crystal structures of the catechol dioxygenase family (EDO), whose active site contains Fe^{II} coordinated with two histidines and one glutamate (Fig. 1). It can be seen from the data presented in Table 2 that the structural characteristics of **1**–**3** depend only slightly on the presence of electron-donating of electron-withdrawing substituents in the ligand. On the whole the bond distances between the iron atom and the nearest donors in complex **4** differ insignificantly from the same parameters of the other model complexes. Note that the difference between Fe—N(2) and Fe—N(3) in **4** is larger than the same difference in the other model complexes and is close to the difference observed in the active site of the EDO enzyme [13].

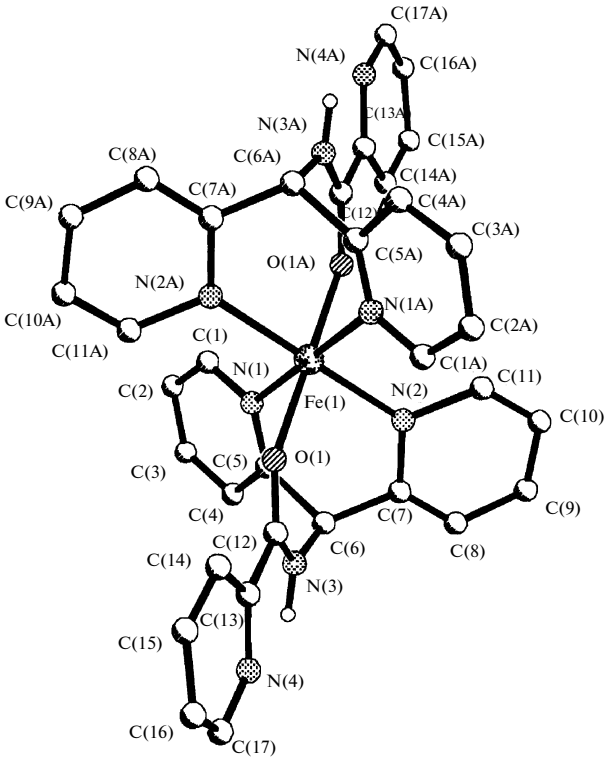

Fig. 3. X-ray structure of complex cation **4**.

The catalytic activity of complex **4** was studied in the oxidation of cyclohexane, 1,2-dimethylcyclohexane, and cyclohexene (Table 3, Fig. 4). It follows from the data presented in Table 3 that the introduction of the electron donor pyridyl into the outer sphere (by substituting pyridyl for phenyl in the carboxamide moiety of the ligand) radically changes the chemoselectivity of the metal complex catalyst. While complex **1** is a very selective catalyst for olefin *cis*-dihydroxylation and is practically inactive even in the oxidation of the weak C—H bond in the allylic position of olefins, the new complex does not catalyze olefin dihydroxylation but is capable of abstracting an H atom from unactivated C—H bonds in stereospecific alkane hydroxylation (Fig. 4). The alcohol : ketone ratio in the catalytic oxidation of cyclohexene with hydrogen peroxide is 2.6, In the hydroxylation of the tertiary bond in *cis*-1,2-dimethylcyclohexane, the resulting alcohol retains the *cis* configuration to the extent of 62%, indicating that the metal complex is involved in oxidation. As is clear from Fig. 5, conversion (product yield on the oxidizer consumption basis) for complex **4**

Table 3. Cyclohexene oxygenation with hydrogen peroxide in an Ar atmosphere catalyzed by complexes **1** and **4** (Fe : H_2O_2 : RH = 1 : X : 1000)

Complex, conditions	Double bond		Allylic α-C–H bond		H_2O_2 conversion, %	Reference
	epoxide, TN	diol, TN	cyclohexenol, TN	cyclohexenone, TN		
1, X = 10, 25°C, 1 h	0	5.6	0.5	0.4	65	[5]
4, X = 50, 20°C, 2 h	4.5	0.1	14	7	51	This work

is only 2 times lower than the conversion for complex **5**, which is an efficient catalyst for alkane oxidation with hydrogen peroxide [9].

The epoxide : diol ratio is commonly correlated with the donor set of the complex [20] and with the spin state of the hydroperoxide intermediate [21]. The *cis*-diol selectivity of the catalyst is attributed to the presence of donating oxygen atoms in the coordination sphere of the metal and/or to the high-spin state of the complex. The catalytic activity and selectivity of complexes **1**–**3** is almost independent on the presence of electron-donating or electron-withdrawing substituents in the ligand [5]. Why does the replacement of phenyl with pyridyl, which leaves the nucleus of the complex intact and has no significant effect on the spectral and structural characteristics of the complex, changes the chemoselectivity of the metal complex catalyst so greatly?

An isotopic study of the mechanism of catalysis of alkene dihydroxylation by complexes **1**–**3** [5] demonstrated that the reaction proceeds via the following $Fe^{II}Fe^{IV}$ catalytic cycle:

$$Fe^{II} + H_2O_2 \rightarrow \eta_2\text{-}Fe^{II} \cdot H_2O_2 \rightarrow \textit{cis}\text{-}Fe^{IV}(OH)_2 + C{=}C \rightarrow Fe^{II} + C(OH){-}C(OH).$$

The involvement of the *cis*-dihydroxyferryl intermediate in olefin *cis*-dihydroxylation was postulated earlier from quantum chemical calculations for another iron(II) complex [22]. The precursor of this intermediate is $\eta_2\text{-}Fe^{II} \cdot H_2O_2$, whose formation needs two labile donor to be located nearby in the coordination sphere of the metal.

At the same time, the catalysis of the hydroxylation of unactivated C–H bonds and epoxidation of double bonds by the model complexes with electron-donating nitrogen atoms is conventionally attributed to the involvement of perferryl intermediates in the $Fe^{III}Fe^{V}$ catalytic cycle [6, 7, 14]:

$$Fe^{III} + H_2O_2 \rightarrow Fe^{III}OOH \rightarrow Fe^{V}{=}O + RH \rightarrow Fe^{III} + ROH.$$

The Fe^{III} complex forms at the initial stage of the reaction via the oxidation of the original complex. The formation of the hydroperoxide intermediate at –40°C in MeCN was reliably established by a number of methods. Because the $Fe^{III}OOH$ intermediate cannot activate strong C–H bonds, it was hypothesized that its heterolytic dissociation yields a perferryl intermediate and the latter is the active oxidizer. The oxoperferryl radical $Fe^{V}{=}O$ has recently been identified by

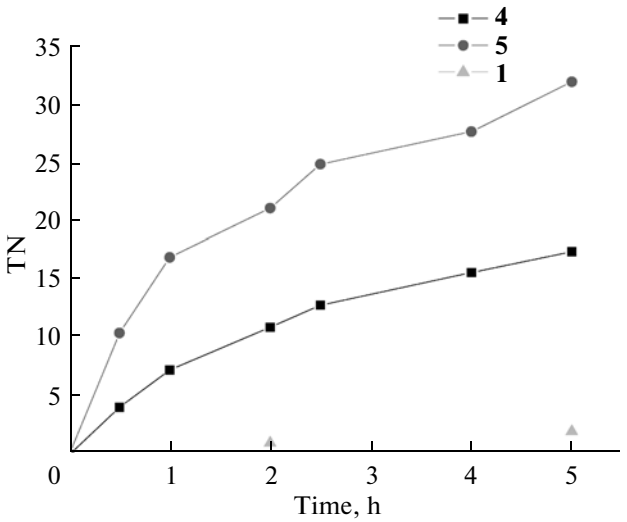

Fig. 4. Kinetics of cyclohexane oxidation catalyzed by complexes **1**, **4**, and **5**.

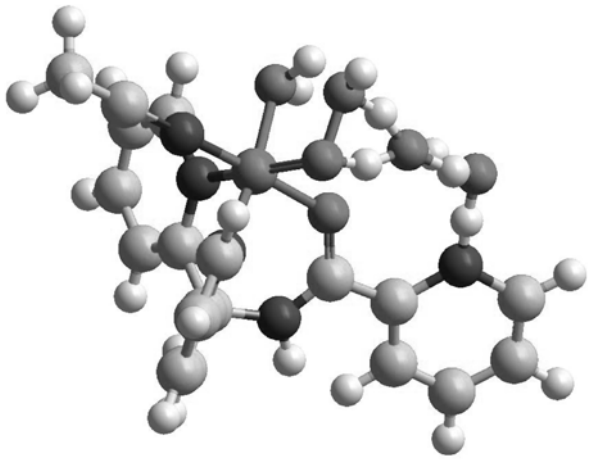

Fig. 5. Hypothetical stabilization of the linear configuration of the peroxide intermediate $\eta_1\text{-}Fe(tpcaH)(H_2O_2)(S)_2 \cdot nH_2O$ by a chain of hydrogen bonds as a result of the inclusion of several water molecules between the peroxide and the outer-sphere pyridyl donor of the ligand.

EPR spectroscopy at −70°C [7]. The observed chemoselectivity of complex **4** is definitely consistent with the $Fe^{III}Fe^{V}$ catalytic cycle. The change in chemoselectivity caused by the replacement of phenyl with pyridyl in the ligand means that the introduction of an outer-sphere donor either hampers the formation of the key intermediate of *cis*-dihydroxylation or facilitates the formation of the key intermediate of olefin epoxidation. Since the *cis*-dihydroxyferryl intermediate apparently stabilizes Fe^{IV} and slows down further iron oxidation, the exclusion of this intermediate from the catalytic cycle is expected to give way to the formation of the more active, perferryl radical. The inhibition of the formation of the *cis*-dihydroxyferryl intermediate might be explained by the absence of labile *cis* monodentate ligands S in the active complex resulting from the solvolysis of the original complex in the catalytic solution. However, according to ^{1}H NMR and mass spectrometric data, the following equilibrium takes place in dilute solutions of complex **4** in MeCH + H_2O: $Fe^{II}(tpcaH)_2 = Fe^{II}(tpcaH)S_3 + tpcaH$. This equilibrium yields a complex in which one of the two facial N,N,O-donor ligands is replaced by solvent molecules. The equilibrium is shifted to the left-hand side for complexes **1**–**3** in dry MeCN [5], while in water, according to ^{1}H NMR data for the similar complex $L_2Fe \cdot 2D_2O$ (**6**), where L is the N,N,O-facial donor ligand 3,3-bis(1-methylimidazol-2-yl)propionate, the same equilibrium is shifted to the right [13].

The solvolytic formation of the complex containing three solvent molecules *cis* to one another in the case of **1**–**3** is confirmed by the observation of oxygen isotope exchange between hydrogen peroxide and water [5], which is possible in the $Fe^{IV}(OH)_2(OH_2)$ intermediate via proton transfer. The hampering of the formation of the η_2-$Fe^{II} \cdot H_2O_2$ intermediate in the presence of two labile *cis* coordination sites may be due to the stabilization of the isomeric intermediate η_1-Fe · H_2O_2, in which the peroxide occupies a single coordination site. This stabilization is possible due to the formation of a bridge consisting of several hydrogen-bonded water molecules between η_1-Fe · H_2O_2 and the outer-sphere pyridyl (Fig. 5). In this case, provided that there is a water molecule in the *cis* position, there can be the heterolytic dissociation of the peroxide bond via proton transfer (Fig. 6a [6, 14]). At the same time, the heterolytic dissociation of the peroxide O–O bond in this structure may be more likely than the homolytic dissociation owing to pyridyl catalyzing proton transfer from the water pool (Fig. 6b). This acid–base catalysis of the heterolytic dissociation of the peroxide bond was observed in both biological [23] and chemical [24] systems.

Thus, the reaction between 2 equiv of the carboxamide ligand tpcaH and Fe^{II} yields the complex $[Fe^{II}(tpcaH)_2]^{2+}$, In this complex, the potentially tetradentate ligand uses its N,N,O-facial donor set in coordination, providing a model for the mononuclear N,N,O-oxygenase family (Fig. 1). The pyridyl that is not coordinated to iron acts as an outer-sphere donor and is apparently involved in the acid–base catalysis of the heterolytic dissociation of the peroxide bond yielding a reactive perferryl intermediate, simulating the same function of the outer-sphere amino acid residues in enzymatic oxidation. Although the exact catalytic mechanism is unknown, it is clear that the outer-sphere donor radically changes the chemoselectivity of the metal complex catalyst, switching the olefin oxygenation process from *cis*-dihydroxylation to epoxidation. At the same time, the presence of an outer-sphere donor markedly enhances the effectiveness of the catalyst, making it possible to hydroxylate unactivated C–H bonds. The important role of outer-sphere noncovalent interactions in the modulation of the strength of the active site is observed both in nature and in biomimetic model systems [25, 26].

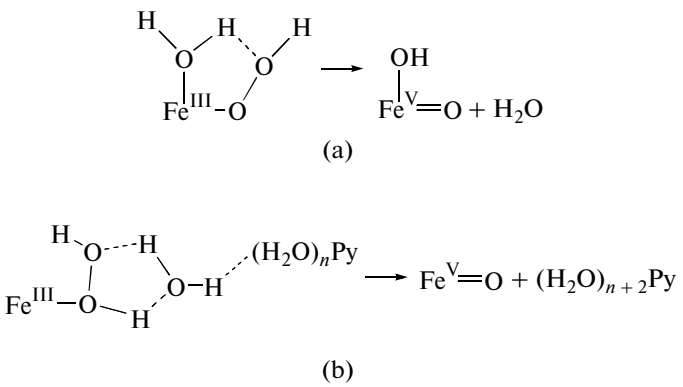

Fig. 6. Possible mechanisms of the heterolytic dissociation of the peroxide bond: (a) mechanism involving a nearest-neighbor water molecule and (b) catalysis by the outer-sphere pyridyl donor involving associated water molecules.

ACKNOWLEDGMENTS

I am grateful to Drs. W.W. Brennessel and V.G. Young, Jr., X-Ray Crystallographic Laboratory, Department of Chemistry, University of Minnesota, for determination of the structure of complex **4** and to Prof. L. Que, Jr. for giving me the opportunity to work in his laboratory.

REFERENCES

1. A. A. Shteinman, Russ. Chem. Rev. **77**, 945 (2008).
2. K. D. Koehntop, J. P. Emerson, and L. Que, Jr., J. Biol. Inorg. Chem. **10**, 87 (2005).
3. P. D. Oldenburg, A. A. Shteinman, and L. Que, Jr., J. Am. Chem. Soc. **127**, 15672 (2005).
4. A. Karlsson, J. V. Parales, R. E. Parales, et al., Science **299**, 1039 (2003).
5. P. D. Oldenburg, Y. Feng, I. Pryjomska-Ray, et al., J. Am. Chem. Soc. **132**, 17713 (2010).
6. A. Bassan, M. R. A. Blomberg, P. E. M. Siegbahn, and L. Que, Jr., Chem. Eur. J. **11**, 692 (2005).

7. O. Y. Lyakin, K. R. Bryliakov, G. J. P. Britovsek, and E. P. Talsi, J. Am. Chem. Soc. **131**, 10798 (2009).
8. J. M. Rowland, M. M. Olmstead, and P. K. Mascharak, Inorg. Chem. **39**, 5326 (2000).
9. E. A. Gutkina, T. B. Rubtsova, and A. A. Shteinman, Kinet. Catal. **44**, 106 (2003).
10. K. S. Hagen, Inorg. Chem. **39**, 5867 (2000).
11. O. A. Mirgorodskaja, A. A. Shevchenko, and A. F. Dodonov, Anal. Chem. **66**, 99 (1994).
12. P. C. A. Bruijnincx, I. L. C. Buurmans, S. Gosiewska, et al., Chem. Eur. J. **14**, 1228 (2008).
13. S. S. Rocks, W. W. Brennessel, T. E. Machonkin, and P. L. Holland, Inorg. Chim. Acta **362**, 1387 (2009).
14. K. Chen and L. Que, Jr., J. Am. Chem. Soc. **123**, 6327 (2001).
15. G. Roelfes, M. Lubben, R. Hage, et al., Chem. Eur. J. **6**, 2152 (2001).
16. S. Zhu, W. W. Brennessel, R. G. Harrison, and L. Que, Jr., Inorg. Chim. Acta **337**, 32 (2002).
17. R. L. Chapmen and K. C. Vagg, Inorg. Chim. Acta **33**, 227 (1979).
18. P. Maslak, J. J. Sczepanski, and M. Parves, J. Am. Chem. Soc. **113**, 1062 (1991).
19. E. I. Solomon, T. C. Brunold, M. I. Davis, et al., Chem. Rev. **100**, 235 (2000).
20. P. D. Oldenburg and L. Que, Jr., J. Mol. Catal. A: Chem. **117**, 15 (2006).
21. K. Chen, M. Costas, J. Kim, et al., J. Am. Chem. Soc. **124**, 3026 (2002).
22. P. Comba, G. Rajaraman, and H. Rohwer, Inorg. Chem. **46**, 3826 (2007).
23. S. L. Newmyer and P. R. Ortiz de Montellano, J. Biol. Chem. **270**, 19430 (1995).
24. L. Feifei, J. England, and L. Que, Jr., J. Am. Chem. Soc. **132**, 2134 (2010).
25. Y. Lu and J. S. Valentine, Curr. Opin. Struct. Biol. **7**, 495 (1997).
26. A. S. Borovik, Acc. Chem. Res. **38**, 54 (2005).